On the Linkage Between Rossby Wave Phase Speed, Atmospheric Blocking, and Arctic Amplification

Jacopo Riboldi, François Lott, Fabio d'Andrea, Gwendal Rivière

On the Linkage Between Rossby Wave Phase Speed, Atmospheric Blocking, and Arctic Amplification

Jacopo Riboldi[1] , François Lott[1] , Fabio D'Andrea[1] , and Gwendal Rivière[1]

[1]Laboratoire de Météorologie Dynamique/IPSL, École Normale Supérieure, PSL Université, Sorbonne Université, École Polytechnique, IP Paris, CNRS, Paris, France

Abstract It has been hypothesized that enhanced Arctic warming with respect to midlatitudes, known as Arctic amplification, had led to a deceleration of eastward propagating Rossby waves, more frequent atmospheric blocking, and extreme weather in recent decades. We employ a novel, daily climatology of Rossby wave phase speed between March 1979 and November 2018, based on upper-level wind data, to test this hypothesis and describe phase speed variability. The diagnostic distinguishes between periods of enhanced or reduced eastward wave propagation and is related to the occurrence of blocking and extreme temperatures over midlatitudes. While remaining tied to the upper-level geopotential gradient, decadal trends in phase speed did not accompany the observed reduction in the low-level temperature gradient. These results confirm the link between low phase speeds and extreme temperature events, but indicate that Arctic amplification did not play a decisive role in modulating phase speed variability in recent decades.

Plain Language Summary The Arctic is warming more rapidly than midlatitudes and the temperature difference between those regions is being reduced. As a result, it has been hypothesized that the jet stream will decrease in intensity and its meanders will move more slowly eastward, leading to more persistent or even extreme weather conditions. As the persistence of weather can substantially vary within and between seasons, assessing long-term changes is not trivial. To tackle this problem, we develop a "weather speedometer" and quantify the west-east displacements of jet meanders over Northern Hemisphere midlatitudes. This metric diagnoses whether jet meanders are on average propagating eastward (positive values), stagnating, or even retrogressing westward (negative values) on each day between March 1979 and November 2018. Using this metric, we confirm that low-speed periods are related to temperature extremes over northern midlatitudes. We also assess that there has not been an overall decrease in the propagation of jet meanders despite the significant reduction of the meridional temperature difference observed in recent decades. Results suggest the need of an improved understanding of the factors determining the persistence of weather conditions and remind caution is needed when attributing recent extreme weather to an increased stagnation of jet stream meanders.

1. Introduction

The Arctic is warming more rapidly than the rest of the globe, a phenomenon known as Arctic amplification (AA: see Cohen et al., 2018 for a review). This phenomenon is due to the interaction of several processes: the observed reduction in sea ice (Dai et al., 2019; Screen & Simmonds, 2010; Taylor et al., 2018), changes in cloud cover and radiative balance over the Arctic (Bintanja et al., 2011; Gong et al., 2017), and anomalous circulation patterns bringing warm, moist air from lower latitudes to the region (Binder et al., 2017; Gimeno et al., 2019; Gong et al., 2020; Papritz, 2020).

According to the most discussed hypothesis, enhanced high-latitude warming would influence midlatitude weather via a systematic increase in amplitude and reduction in the phase speed of Rossby waves. This effect would be due to a reduction of the Arctic-to-midlatitude geopotential gradient and by changes in the configuration of the jet stream (Francis & Vavrus, 2012; Ronalds et al., 2018). Rossby waves would then propagate more slowly eastward, increasing the stationarity of flow patterns related to weather extremes (Chen & Luo, 2019; Coumou et al., 2014; Hoskins & Woollings, 2015; Screen & Simmonds, 2014), including heatwaves in summer and cold spells in winter.

Despite the documented correlation between Arctic warming and midlatitude extreme weather events (Cohen et al., 2018; Francis & Vavrus, 2012; Kug et al., 2015), a clear causal link between the two has not been established yet (Barnes, 2013; Barnes et al., 2014; Barnes & Polvani, 2015; Cohen et al., 2014, 2019; Francis, 2017; Overland, 2016; Screen et al., 2018). Recent studies even suggest that anomalous high-latitude warming might be an effect, rather than the cause, of planetary-scale circulation patterns leading to midlatitude temperature extremes (Blackport et al., 2019; Blackport & Screen, 2020; Gong et al., 2020; McCusker et al., 2016; Meleshko et al., 2016; Wang et al., 2020). However, despite such fundamental uncertainties, the hypothesis that AA has led or will lead to an increased frequency of weather extremes still prevails in divulgation and dissemination papers (Alfred Wegener Institute, H. C. P. & Marine Research, 2019; Francis, 2018; Hamilton & Lemcke-Stampone, 2014; Katz, 2019; McSweeney, 2019).

Several observational and modeling studies focused on possible changes in Rossby wave amplitude following AA, obtaining inconsistent results with respect to the employed amplitude metric (Barnes, 2013; Blackport & Screen, 2020; Francis & Vavrus, 2012, 2015; Screen & Simmonds, 2013; Screen et al., 2018; Sussman et al., 2020; Vavrus et al., 2017). The recent study by Blackport and Screen (2020) concluded, using a combination of observational and model-based evidence, that AA did not significantly affect the amplitude of Rossby waves. The same study did not exclude, however, that AA could make Rossby waves slower.

Fewer studies have investigated possible changes in the eastward propagation of Rossby waves in relation to AA. Two main approaches have been employed: the direct calculation of phase speed estimates (Barnes, 2013; Barnes & Polvani, 2015; Coumou et al., 2015; Domeisen et al., 2018) and the use of proxies indirectly related to phase speed, like teleconnections (e.g., the Arctic Oscillation), atmospheric blocking or the zonally averaged zonal wind in the middle to upper troposphere (Barnes et al., 2014; Hassanzadeh & Kuang, 2015; Li & Luo, 2019). Barnes (2013) employed space/time spectral analysis to highlight the absence of robust phase speed trends for planetary ($n = 1$–6) waves over the North Atlantic between 1980 and 2011; furthermore, the author noticed that phase speed and zonal wind trends did not necessarily have the same sign, especially in summer. Coumou et al. (2015) focused on boreal summer and also confirmed the absence of significant phase speed trends (except for the $n = 10$ wave number), using an alternative phase speed metric that, however, was based on a spectral analysis that did not explicitly separate fast from slow waves. Both these studies did not specifically link the developed phase speed metric to the circulation features causing extreme weather over midlatitudes, as atmospheric blocking and Rossby wave packets (Fragkoulidis & Wirth, 2020; Röthlisberger & Martius, 2019; Röthlisberger et al., 2019; Wirth et al., 2018). Methods employing indirect phase speed proxies, on the other hand, encountered difficulties related to the large interannual variability of the extratropical flow (Barnes et al., 2014) and to causality attribution, as it is not clear whether, for example, atmospheric blocking arises because of reduced eastward wave propagation or vice versa (Hassanzadeh & Kuang, 2015).

The present study explores how intraseasonal circulation patterns at the synoptic/weekly time scale influence the interannual phase speed variability, helping to contextualize decadal phase speed trends. Employing a spectral-based phase speed diagnostic able to properly represent Rossby wave characteristics at different time scales, we investigate the evolution and the variability of phase speed in the last 40 years and assess whether AA was associated with decadal phase speed trends over midlatitudes. The first part of this study delineates the relationship between direct phase speed estimates and indirect phase speed proxies, by studying the circulation, blocking anomalies, and extreme temperatures associated with high and low phase speeds in each season. The second part is dedicated to a detailed trend analysis, updated to 2018, to understand the drivers of phase speed variability in recent decades of AA.

2. Phase Speed Diagnostic

The midlatitude flow can be described as a superposition of waves across a broad range of frequencies and wave numbers, and the phase speed of each wave results from the ratio of the two. Therefore, building a global phase speed metric presupposes the knowledge of the spatial and temporal Rossby wave evolution over a given period of time. To obtain that, we perform a time/space spectral decomposition of the meridional wind at 250 hPa, approximately the level of the jet stream, along each latitude circle between 35°N and 75°N across the ERA-Interim reanalysis data set (March 1979 to November 2018). Each date is associated with a time window of 61 days centered on the day of interest. Over this window, the signal is decomposed using a double Fourier transform onto a sum of harmonics with a-dimensional wave number n and angular

frequency ω. For each latitude, the periodogram constituted by the square of the Fourier coefficients (Figure S1a in the supporting information) is interpolated in the phase speed (c_p) domain (Domeisen et al., 2018; Randel & Held, 1991). An estimate of the spectrum is finally obtained by averaging the interpolated periodograms across latitude (Figure S1b).

A global estimate of the phase speed is then obtained by doing a weighted average of the phase speeds of each harmonic in the range $n = 1$–15: the weights are the corresponding values of the spectrum, indicating which harmonics (n, c_p) dominate the flow in the considered time window. Previous studies considered smaller wave number ranges (e.g., $n = 1$–6), but in principle there is no reason to expect that eventual changes in wave propagation would affect only low wave numbers. More details about spectral decomposition and phase speed computation are given in the supporting information Text S2.

The planetary scale patterns related to high and low phase speeds are investigated by compositing the 250 hPa-geopotential anomalies of the days in the top 5% and bottom 5% of phase speed values in each winter and summer (Figure 1). Dates and values of phase speed maxima and minima for each season are listed in the supporting information Tables S1 and S2, while anomaly computation and significance testing are described in Text S3. Days of high phase speed during DJF are related to an enhanced meridional geopotential gradient over midlatitudes, that becomes particularly pronounced at the eastern edge of the Pacific and Atlantic storm track regions: this is indicated by a stronger than normal upper-level zonal wind (Figure 1a). Conversely, periods of low phase speed feature positive geopotential anomalies at high latitudes, with two separate maxima at the end of the storm tracks, and an overall reduction of the meridional geopotential gradient and zonal wind over midlatitudes (Figure 1b). A similar picture is obtained for boreal summer, especially in the North Atlantic sector: the composite features weaker geopotential and zonal wind anomalies, albeit of the same sign as in DJF (Figures 1c and 1d). Individual periods of high and low phase speed, centered around relative maxima and minima of the phase speed time series, have been analyzed singularly to ensure that the circulation patterns actually correspond to progressive or stationary waves (Figure S2). Days with winter low phase speed indeed feature isolated, westward propagating waves associated with anticyclonic anomalies at high latitudes (55–75°N), likely related to atmospheric blocking events (Figures S2c and S2e).

3. Linkage With Blocking and Temperature Extremes

Since configurations of stationary and amplified flow are often associated with blocking and extreme temperature events (Fragkoulidis et al., 2018; Röthlisberger et al., 2016, 2019; Screen & Simmonds, 2014), we analyzed composites of daily blocking frequency anomaly for the days in the seasonal top 5% and bottom 5% of phase speed (4 days in each season; Figures 2a, 2b, 2d, and 2e). Blocking frequency, computed employing the Schwierz et al. (2004) diagnostic, is defined at each grid point as the ratio between the number of blocked days and the total number of considered days, while anomalies are computed with respect to the respective seasonal mean. We notice that DJF days with high phase speed are characterized by a general diminution of blocking activity with respect to climatology, with the exception of a few positive blocking frequency anomalies over the west Pacific (Figure 2a). The opposite pattern is observed for low phase speed days, with enhanced blocking occurrence, especially at the northern end of the storm tracks (Figure 2b). The same observations hold during JJA, with increased (decreased) high-latitude blocking during periods of low (high) phase speed (Figures 2d and 2e). This relationship can be understood when picturing blocking as a persistent, large-scale anticyclonic flow anomaly: high-latitude blocking is related to easterlies over midlatitudes, that reduce the strength of the midlatitude westerlies and displace them equatorward. The suppression/enhancement of blocking activity during high/low phase speed days remains visible employing the Davini et al. (2012) and Woollings et al. (2018) blocking diagnostics (cf. Figures S3 and S4 and Text S4).

The link between phase speed and extreme events is discussed using the midlatitude extreme index (MEX) introduced by Coumou et al. (2014), that provides a global measure of the temperature variance over Northern Hemisphere midlatitudes (35–75°N in this study; MEX calculation is described in Text S5). High values of MEX correspond to widespread 2-m temperature standardized anomalies, both cold and warm, over the considered region; conversely, low values of the index indicate smaller than normal anomalies. Days of low DJF phase speed feature significantly higher MEX values than high phase speed days (Figure 2c; t test on the mean of MEX logarithm, $p < 0.01$). Conversely, periods of rapidly propagating waves are linked to significantly fewer temperature extremes than climatology. Consistent results emerge for boreal summer
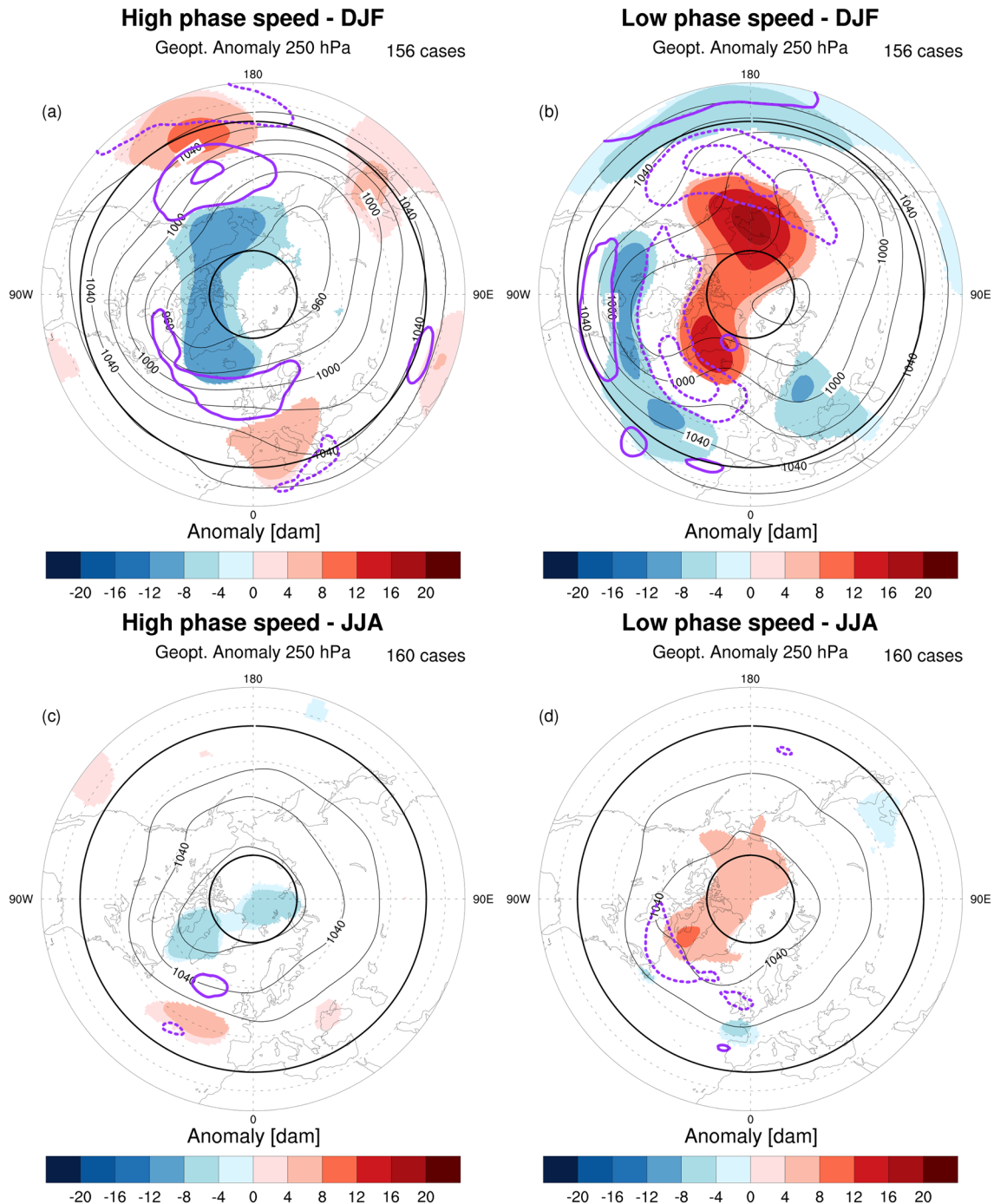
Figure 1. High and low phase speed days Composite of 250 hPa geopotential heights (black contours, between 940 dam and 1,060 dam every 20 dam) and zonal wind anomalies (purple contours, only −10, −5, +5, +10 m s^{-1} isotachs, negative contours dashed) associated with the days in the (a) top 5% and (b) bottom 5% of phase speed values in each of the 39 winters between 1979/1980 and 2017/2018. Significant anomalies (top 1%) with respect to the bootstrapped null distribution are shaded, according to the color scale. (c, d) Same as above, but relative to the 40 boreal summers between 1979 and 2018. Black bold circles indicate the 35°N and 75°N parallel.
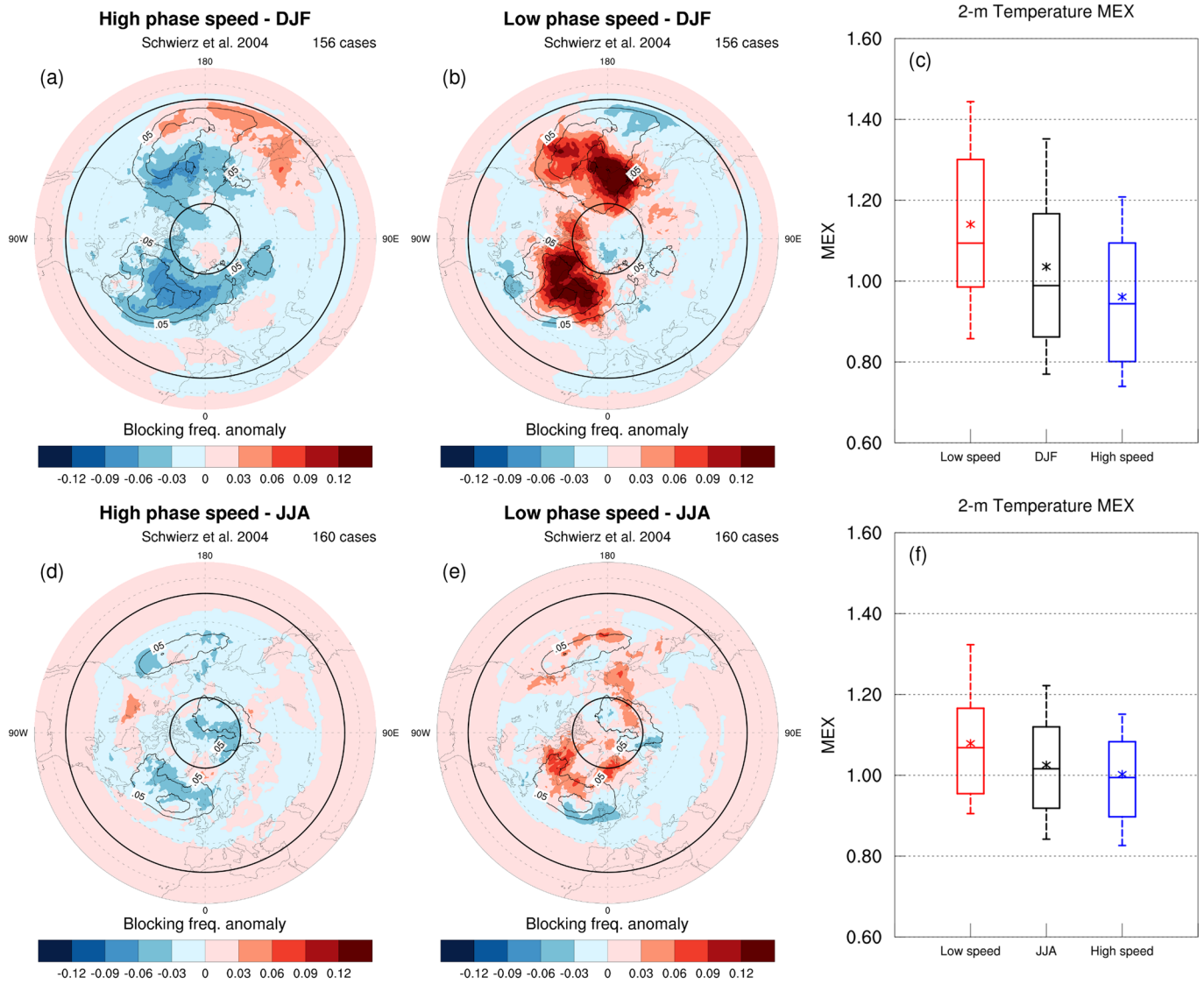
Figure 2. Low phase speeds are related to blocking and extreme temperatures. Composite of blocking frequency anomalies during the days in the (a) top 5% and (b) bottom 5% of phase speed values in each of the 39 winters between 1979/1980 and 2017/2018. Climatological blocking frequency is indicated by the black solid lines (starting from 0.05, every 0.05). (c) Box-and-whiskers diagrams of 2-m temperature MEX values for the same subsets of bottom 5% (red) and top 5% (blue) phase speed days, with the DJF MEX distribution plotted for reference (black). The line in each box marks the median value, while the star marks the mean value. The lower (upper) whisker marks the lower (upper) decile of each distribution, while the lower (upper) bound of the box shows the lower (upper) quartile. (d–f) Same as (a–c), but relative to the 40 boreal summers between 1979 and 2018. Black bold circles indicate the 35°N and 75°N parallel.
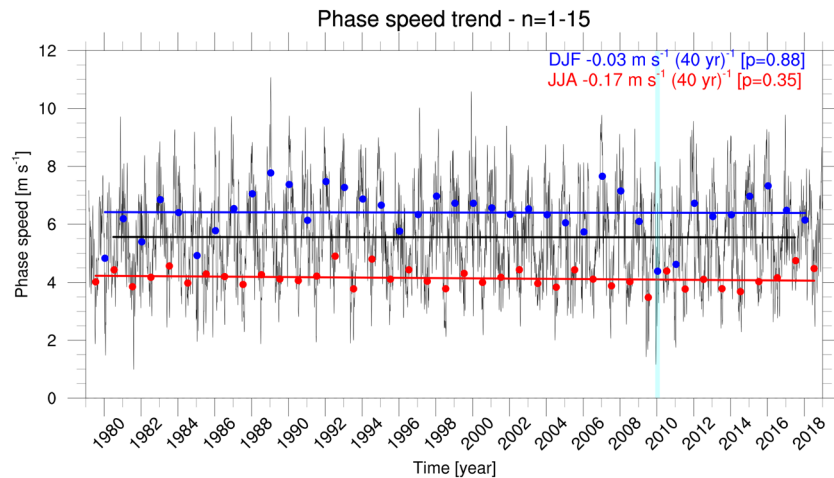
Figure 3. Variability of phase speed in the latest 40 years. Evolution of phase speed related to the total ($n = 1$–15) wave range for all days between March 1979 and November 2018 (black thin line). Blue dots correspond to values of average DJF phase speed, red dots to average JJA phase speed. Thick lines correspond to linear regression for yearly (black), DJF (blue), and JJA (red) means. The light blue vertical stripe highlights the 2009/2010 winter.

(Figure 2f), confirming the link between reduced eastward propagation of Rossby waves and extreme temperatures, also pointed out by previous work about quasi-resonant Rossby wave amplification (Kornhuber, Comou, et al., 2019; Kornhuber, Osprey, et al., 2019).

4. Trend Analysis and Link With Arctic Amplification

The daily and seasonal evolution of phase speed shows a large variability (Figure 3). Rossby waves tend to propagate faster eastward in winter than in summer, and this is likely due to the different strengths of the background flow. A notable low-speed event is winter 2009/2010, that features the absolute minimum in seasonally averaged winter phase speed ($c = 4.38$ m s^{-1}, highlighted in light blue in Figure 3) in the whole data set. That winter, characterized by extremely negative values of the Arctic oscillation index, featured particularly harsh conditions and repeated cold spells over North America and Europe (Jung et al., 2011; Sprenger et al., 2017).

Trend analysis, performed using the Theil-Sen linear trend estimate and the Mann-Kendall significance test, shows that no significant phase speed trend has emerged from the year-to-year variability during the last 40 years, neither in the yearly mean (-0.015 m s^{-1} (40 yr)$^{-1}$, $p = 0.90$) nor when considering winter and summer seasonal averages (Figure 3). The absence of trend is confirmed when considering estimates of phase speed drawn separately from the planetary ($n = 1$–6) and synoptic ($n = 7$–15) portion of the spectrum (Figure S5). No significant trend is found even if maxima or minima of phase speed over consecutive 7-day or 14-day time periods are considered (Figure S6; the duration of 7 days corresponds to the decorrelation time of the phase speed time series). Finally, the time distance between high and low phase speed periods (lasting at least seven consecutive days above/below the 90th/10th percentile) does not exhibit significant trends either, indicating that such events have not become more or less frequent in recent decades (Figure S7).

We investigate now, using two different metrics, the relationship between the phase speed metric and AA. The first metric considers the difference in 850 hPa temperature between middle (35–65°N) and high latitudes (65–90°N), a quantity that significantly decreased in the latest 39 winters because of AA (Figure S8a). The second metric evaluates the difference in 250 hPa geopotential anomalies between the same latitudinal bands, trying to highlight the upper-level effect of the low-level temperature increase: this quantity exhibits a negative, but nonsignificant trend during DJF (Figure S8b). The phase speed metric is strongly correlated (+0.62 Pearson correlation coefficient) with the meridional difference of 250 hPa geopotential throughout the whole year (see Table S3), and correlated to a lesser extent (+0.48) with the 850 hPa temperature difference.

Given that AA emerged in recent decades, we examine also phase speed trends over shorter time periods (Figure 4). Two main sets of significantly negative ($p < 0.05$) phase speed trends are visible for DJF,
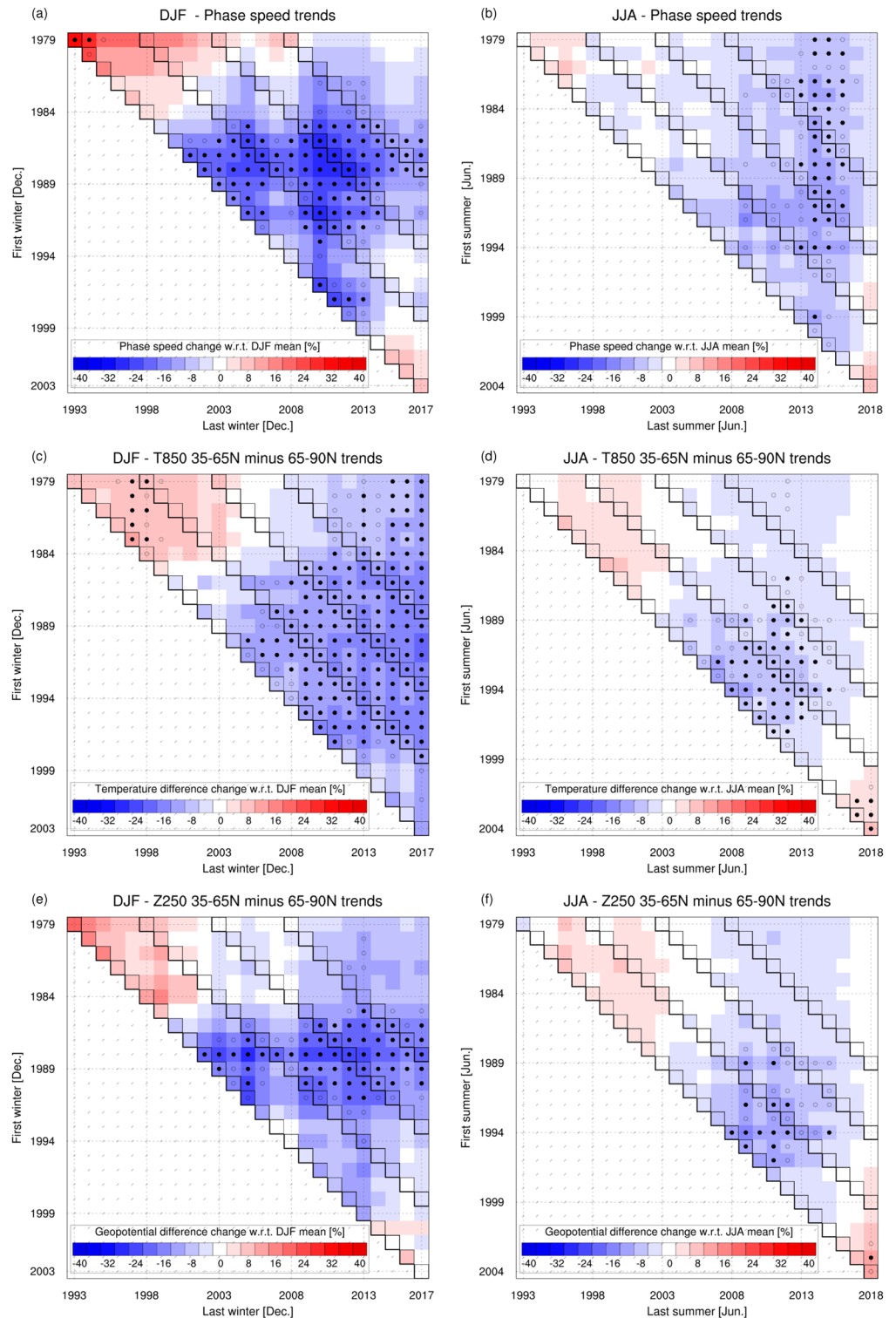
Figure 4. Short-term trends of phase speed and AA, (a) DJF trends in phase speed metric as a function of start year (vertical axis) and end year (horizontal axis), expressed as the integrated phase speed change over the considered time interval with respect to the seasonal mean phase speed value. Only trends computed from time intervals longer than 15 years are plotted. Stippling (open circles) indicates statistically significant trends at the 95% (90%) confidence level. (b) As in (a), but for JJA. (c, d) As in (a, b), but for trends in zonally averaged 850 hPa temperature difference (35–65°N minus 65–90°N). (e, f) As in (c, d), but for trends in zonally averaged 250 hPa geopotential difference (35–65°N minus 65–90°N). In DJF plots, the initial and final years refer to December: for instance, the values corresponding to 1979 refer to trends starting in winter 1979/1980.

both referring to time intervals starting between 1986 and 1992. The first one corresponds to short-lived (15 to 20 years) trends ending before winter 2006/2007, in periods with no significant temperature difference trend (Figures 4a and 4c); the second one corresponds to longer periods (around 25–30 years) ending between winters 2009/2010 and 2017/2018. Although the Theil-Sen trend estimator is less sensitive to outliers than other methods, it should be noticed that high values of seasonally averaged phase speed were recorded between winters 1987/1988 and 1992/1993 (Figure 3) and this likely contributes to the negative trends mostly starting in this time period. Notably, no significant long-term phase speed trend is visible in periods starting after winter 1993/1994, despite the significant AA observed since. The absence of a strong association between Arctic-to-midlatitude temperature difference trends and phase speed trends is an evidence toward the conclusion that the former did not drive the latter.

On the other hand, significant trends in upper-level geopotential difference cooccur more precisely with phase speed trends than with low-level temperature difference trends (Figure 4e). This is consistent with the higher correlation existing between phase speed and meridional geopotential difference, and with the fact that high (low) phase speeds occur during periods of increased (decreased) meridional geopotential gradient at upper levels, as previously discussed. While long-term geopotential increase due to global warming is observed everywhere (Figure S9a), periods of significant negative trends in geopotential gradient correspond to a temporary weakening of the positive trend at low latitudes only (between 35°N and 65°N; see Figures S9b and S9c): this highlights the potential role of non-Arctic processes in modulating phase speed variability.

During summer, weak but significant negative phase speed trends are observed for periods with ending years between 2013 and 2016, regardless of the starting year (Figure 4b). Interestingly, these negative trends do not cooccur with periods of significant negative reductions of temperature and geopotential gradient (Figures 4d and 4f). It is therefore unlikely that the evolution of the Arctic-to-midlatitude temperature gradient drove such trends. In addition, the fact that AA is mostly a winter phenomenon and that during summer the midlatitude waveguide is less defined and intermittent, makes less grounded the hypothesis of a link between AA and phase speed reduction in the warm season.

5. Summary and Open Points

A newly developed, spectral-based metric indicates that there has not been a systematic diminution in the phase speed of Rossby waves over the Northern Hemisphere in the last 40 years. Intermittent negative trends have been observed in selected periods between 1988 and 2017, in winter as well as in summer: they have been associated with a contextual reduction of the meridional geopotential gradient at upper levels during winter, but not necessarily with a concomitant reduction of the low-level temperature gradient. These observations do not support the hypothesis that the low-level reduction of the meridional temperature gradient, due to AA, has led to a reduction in the phase speed of Rossby waves. On the other hand, it is shown that periods of reduced Rossby wave phase speed are systematically related to atmospheric blocking and temperature extremes, regardless of AA. These results highlight the role of the interannual and intraseasonal variability of phase speed in inducing extreme weather across seasons, rather than of a long-term phase speed reduction linked to AA.

The short-term, negative phase speed trends observed during DJF occur in time periods featuring also positive trends of Rossby wave amplitude, as assessed by Blackport and Screen (2020) (see their Figure 2c). The same study concluded that such amplitude trends resulted from interannual variability, and that wave activity modulated the meridional temperature gradient during those periods rather than the opposite. These results cannot be simply applied to the present analysis of phase speed, but the decoupling between intermittent trends in geopotential gradient and multidecadal trends in low-level temperature gradient suggest that the latter is not sufficient to explain the observed decadal phase speed variations.

This decoupling between trends in meridional upper-level geopotential gradient and low-level temperature gradient is not surprising. First of all, upper-level geopotential evolution is governed by a complex budget between processes happening in the whole atmospheric column, as detailed by the quasi-geostrophic geopotential tendency equation, and by the effect of diabatically induced a-geostrophic circulations (Holton, 2004; Steenburgh & Holton, 1993). This consideration indicates the need of detailed dynamical diagnostics to precisely constrain the effects of AA on the upper tropospheric flow. In addition, poleward moving extratropical cyclones can lead to anomalous heat and moisture transport to the Arctic without a pronounced reversal

of the meridional geopotential gradient (Binder et al., 2017; Hong et al., 2020; Perlwitz et al., 2015; Wang et al., 2020; Wernli & Papritz, 2018).

Finally, this study did not explicitly address the potential role of upper-level warming in tropical regions, that may counteract the effects of AA on the jet stream in the so-called "tug-of-war" (Barnes & Polvani, 2015; Screen et al., 2018). A preliminary analysis indicates that short-term phase variability in meridional geopotential gradient at upper levels was mostly driven by lower latitudes, while Arctic geopotential increased steadily (Figure S9). Performing sensitivity runs in general circulation models with prescribed forcing can make the drivers of phase speed variability more explicit.

Data Availability Statement

The analysis has been conducted using the ERA-Interim reanalysis data set, available at ECMWF (https://www.ecmwf.int/en/forecasts/datasets/reanalysis-datasets/era-interim).

References

Alfred Wegener Institute, H. C. P., & Marine Research (2019). A warming Arctic produces weather extremes in our latitudes. https://www.sciencedaily.com/releases/2019/05/190528140115.htm

Barnes, E. A. (2013). Revisiting the evidence linking Arctic amplification to extreme weather in midlatitudes. *Geophysical Research Letters*, *40*, 4734–4739. https://doi.org/10.1002/grl.50880

Barnes, E. A., Dunn-Sigouin, E., Masato, G., & Woollings, T. (2014). Exploring recent trends in Northern Hemisphere blocking. *Geophysical Research Letters*, *41*, 638–644. https://doi.org/10.1002/2013GL058745

Barnes, E. A., & Polvani, L. M. (2015). CMIP5 projections of Arctic amplification, of the North American/North Atlantic circulation, and of their relationship. *Journal of Climate*, *28*, 5254–5271. https://doi.org/10.1175/JCLI-D-14-00589.1

Binder, H., Boettcher, M., Grams, C. M., Joos, H., Pfahl, S., & Wernli, H. (2017). Exceptional air mass transport and dynamical drivers of an extreme wintertime Arctic warm event. *Geophysical Research Letters*, *44*, 12,028–12,036. https://doi.org/10.1002/2017GL075841

Bintanja, R., Graversen, R., & Hazeleger, W. (2011). Arctic winter warming amplified by the thermal inversion and consequent low infrared cooling to space. *Nature Geoscience*, *4*, 758–761. https://doi.org/10.1038/ngeo1285

Blackport, R., & Screen, J. A. (2020). Insignificant effect of Arctic amplification on the amplitude of midlatitude atmospheric waves. *Science Advances*, *6*. https://doi.org/10.1126/sciadv.aay2880

Blackport, R., Screen, J. A., van der Wiel, K., & Bintanja, R. (2019). Minimal influence of reduced Arctic sea ice on coincident cold winters in mid-latitudes. *Nature Climate Change*, *9*, 697–704. https://doi.org/10.1038/s41558-019-0551-4

Chen, X., & Luo, D. (2019). Winter midlatitude cold anomalies linked to North Atlantic sea ice and SST anomalies: The pivotal role of the potential vorticity gradient. *Journal of Climate*, *32*, 3957–3981. https://doi.org/10.1175/JCLI-D-18-0504.1

Cohen, J., Pfeiffer, K., & Francis, J. A. (2018). Warm Arctic episodes linked with increased frequency of extreme winter weather in the United States. *Nature Communications*, *9*, 869. https://doi.org/10.1038/s41467-018-02992-9

Cohen, J., Screen, J. A., Furtado, J. C., Barlow, M., Whittleston, D., Comou, D., et al. (2014). Recent Arctic amplification and extreme mid-latitude weather. *Nature Geoscience*, *7*, 627–637. https://doi.org/10.1038/ngeo2234

Cohen, J., Zhang, X., Francis, J., Jung, T., Kwok, R., Overland, J., et al. (2019). Divergent consensuses on Arctic amplification influence on midlatitude severe winter weather. *Nature Climate Change*, *10*, 20–29. https://doi.org/10.1038/s41558-019-0662-y

Cohen, J., Zhang, X., Francis, J., Jung, T., Kwok, R., Overland, J., et al. (2018). Arctic change and possible influence on mid-latitude climate and weather: A US CLIVAR white paper (*No. 2018-1*). Washington, DC: U.S. CLIVAR Project Office. https://doi.org/10.5065/D6TH8KGW

Coumou, D., Lehmann, J., & Beckmann, J. (2015). The weakening summer circulation in the Northern Hemisphere mid-latitudes. *Science*, *348*, 324–327. https://doi.org/10.1126/science.1261768

Coumou, D., Petoukhov, V., Rahmstorf, S., Petri, S., & Schellnhuber, H. J. (2014). Quasi-resonant circulation regimes and hemispheric synchronization of extreme weather in boreal summer. *Proceedings of the National Academy of Sciences*, *111*, 12,331–12,336. https://doi.org/10.1073/pnas.1412797111

Dai, A., Luo, D., Song, M., & Lu, J. (2019). Arctic amplification is caused by sea-ice loss under increasing CO_2. *Nature Communications*, *10*, 99–115. https://doi.org/10.1038/s41467-018-07954-9

Davini, P., Cagnazzo, C., Gualdi, S., & Navarra, A. (2012). Bidimensional diagnostics, variability, and trends of Northern Hemisphere blocking. *Journal of Climate*, *25*, 6496–6509. https://doi.org/10.1175/JCLI-D-12-00032.1

Domeisen, D. I. V., Martius, O., & Jiménez-Esteve, B. (2018). Rossby wave propagation into the Northern Hemisphere stratosphere: The role of zonal phase speed. *Geophysical Research Letters*, *45*, 2064–2071. https://doi.org/10.1002/2017GL076886

Fragkoulidis, G., & Wirth, V. (2020). Local Rossby wave packet amplitude, phase speed, and group velocity: Seasonal variability and their role in temperature extremes. *Journal of Climate*, *33*, 8767–8787. https://doi.org/10.1175/JCLI-D-19-0377.1

Fragkoulidis, G., Wirth, V., Bossmann, P., & Fink, A. H. (2018). Linking Northern Hemisphere temperature extremes to Rossby wave packets. *Quarterly Journal of the Royal Meteorological Society*, *144*, 553–566. https://doi.org/10.1002/qj.3228

Francis, J. A. (2017). Why are Arctic linkages to extreme weather still up in the air? *Bulletin of the American Meteorological Society*, *98*, 2551–2557. https://doi.org/10.1175/BAMS-D-17-0006.1

Francis, J. A. (2018). Meltdown. *Scientific American*, *318*, 48–53. https://doi.org/10.1038/scientificamerican0418-48

Francis, J. A., & Vavrus, S. J. (2012). Evidence linking Arctic amplification to extreme weather in mid-latitudes. *Geophysical Research Letters*, *39*, L06801. https://doi.org/10.1029/2012GL051000

Francis, J. A., & Vavrus, S. J. (2015). Evidence for a wavier jet stream in response to rapid Arctic warming. *Environmental Research Letters*, *10*, 14005. https://doi.org/10.1088/1748-9326/10/1/014005

Gimeno, L., Vázquez, M., Eiras-Barca, J., Sorí, R., Algarra, I., & Nieto, R. (2019). Atmospheric moisture transport and the decline in Arctic sea ice. *Wiley Interdisciplinary Reviews: Climate Change*, *10*, e588. https://doi.org/10.1002/wcc.588

Gong, T., Feldstein, S., & Lee, S. (2017). The role of downward infrared radiation in the recent Arctic winter warming trend. *Journal of Climate*, *30*, 4937–4949. https://doi.org/10.1175/JCLI-D-16-0180.1

Gong, T., Feldstein, S. B., & Lee, S. (2020). Rossby wave propagation from the Arctic into the midlatitudes: Does it arise from in situ latent heating or a trans-Arctic wave train? *Journal of Climate*, *33*, 3619–3633. https://doi.org/10.1175/JCLI-D-18-0780.1

Hamilton, L. C., & Lemcke-Stampone, M. (2014). Arctic warming and your weather: Public belief in the connection. *International Journal of Climatology*, *34*, 1723–1728. https://doi.org/10.1002/joc.3796

Hassanzadeh, P., & Kuang, Z. (2015). Blocking variability: Arctic amplification versus Arctic oscillation. *Geophysical Research Letters*, *42*, 8586–8595. https://doi.org/10.1002/2015GL065923

Holton, J. (2004). *An introduction to dynamic meteorology* (4th ed., Vol. 88). International Geophysics. Burlington MA: Elsevier Academic Press.

Hong, J., Kim, B., Baek, E., Kim, J., Zhang, X., & Kim, S. (2020). A critical role of extreme Atlantic windstorms in Arctic warming. *Asia-Pacific Journal of Atmospheric Sciences*, *56*, 17–28. https://doi.org/10.1007/s13143-019-00123-y

Hoskins, B., & Woollings, T. (2015). Persistent extratropical regimes and climate extremes. *Current Climate Change Reports*, *1*, 115–124. https://doi.org/10.1007/s40641-015-0020-8

Jung, T., Vitart, F., Ferranti, L., & Morcrette, J.-J. (2011). Origin and predictability of the extreme negative NAO winter of 2009/10. *Geophysical Research Letters*, *38*, L07701. https://doi.org/10.1029/2011GL046786

Katz, C. (2019). Warming at the poles will soon be felt globally in rising seas, extreme weather. *National Geographic*. https://www.nationalgeographic.com/science/2019/12/arctic/

Kornhuber, K., Comou, D., Vogel, E., Lesk, C., Donges, J. F., Lehmann, J., & Horton, R. M. (2019). Amplified Rossby waves enhance risk of concurrent heatwaves in major breadbasket regions. *Nature Climate Change*, *10*, 48–53. https://doi.org/10.1038/s41558-019-0637-z

Kornhuber, K., Osprey, S., Coumou, D., Petri, S., Petoukhov, V., Rahmstorf, S., & Gray, L. (2019). Extreme weather events in early summer 2018 connected by a recurrent hemispheric wave-7 pattern. *Environmental Research Letters*, *14*, 54002. https://doi.org/10.1088/1748-9326/ab13bf

Kug, J.-S., Jeong, J.-H., Jang, Y.-S., Kim, B.-M., Folland, C. K., Min, S.-K., & Son, S.-W. (2015). Two distinct influences of Arctic warming on cold winters over North America and East Asia. *Nature Geoscience*, *8*, 759–762. https://doi.org/10.1038/ngeo2517

Li, M., & Luo, D. (2019). Winter Arctic warming and its linkage with midlatitude atmospheric circulation and associated cold extremes: The key role of meridional potential vorticity gradient. *Science China Earth Sciences*, *62*, 1329–1339. https://doi.org/10.1007/s11430-018-9350-9

McCusker, K. E., Fyfe, J. C., & Sigmond, M. (2016). Twenty-five winters of unexpected Eurasian cooling unlikely due to Arctic sea-ice loss. *Nature Geoscience*, *9*, 838–842. https://doi.org/10.1038/ngeo2820

McSweeney, R. (2019). How is Arctic warming linked to the polar vortex and other extreme weather? https://www.carbonbrief.org/qa-how-is-arctic-warming-linked-to-polar-vortext-other-extreme-weather

Meleshko, V. P., Johannessen, O. M., Baidin, A. V., Pavlova, T. V., & Govorkova, V. A. (2016). Arctic amplification: Does it impact the polar jet stream? *Tellus A*, *68*, 32330. https://doi.org/10.3402/tellusa.v68.32330

Overland, J. E. (2016). A difficult Arctic science issue: Midlatitude weather linkages. *Polar Science*, *10*, 210–216. https://doi.org/10.1016/j.polar.2016.04.011

Papritz, L. (2020). Arctic lower-tropospheric warm and cold extremes: Horizontal and vertical transport, diabatic processes, and linkage to synoptic circulation features. *Journal of Climate*, *33*, 993–1016. https://doi.org/10.1175/JCLI-D-19-0638.1

Perlwitz, J., Hoerling, M., & Dole, R. (2015). Arctic tropospheric warming: Causes and linkages to lower latitudes. *Journal of Climate*, *28*, 2154–2167. https://doi.org/10.1175/JCLI-D-14-00095.1

Randel, W. J., & Held, I. M. (1991). Phase speed spectra of transient eddy fluxes and critical layer absorption. *Journal of the Atmospheric Sciences*, *48*, 688–697. https://doi.org/10.1175/1520-0469(1991)048h0688:PSSOTEi2.0.CO;2

Ronalds, B., Barnes, E., & Hassanzadeh, P. (2018). A barotropic mechanism for the response of jet stream variability to Arctic amplification and sea ice loss. *Journal of Climate*, *31*, 7069–7085. https://doi.org/10.1175/JCLI-D-17-0778.1

Röthlisberger, M., Frossard, L., Bosart, L. F., Keyser, D., & Martius, O. (2019). Recurrent synoptic-scale Rossby wave patterns and their effect on the persistence of cold and hot spells. *Journal of Climate*, *32*, 3207–3226. https://doi.org/10.1175/JCLI-D-18-0664.1

Röthlisberger, M., & Martius, O. (2019). Quantifying the local effect of Northern Hemisphere atmospheric blocks on the persistence of summer hot and dry spells. *Geophysical Research Letters*, *46*, 10,101–10,111. https://doi.org/10.1029/2019GL083745

Röthlisberger, M., Pfahl, S., & Martius, O. (2016). Regional-scale jet waviness modulates the occurrence of midlatitude weather extremes. *Geophysical Research Letters*, *43*, 989–997. https://doi.org/10.1002/2016GL070944

Schwierz, C., Croci-Maspoli, M., & Davies, H. C. (2004). Perspicacious indicators of atmospheric blocking. *Geophysical Research Letters*, *31*, L06125. https://doi.org/10.1029/2003GL019341

Screen, J. A., Deser, C., Smith, D. M., Zhang, X., Blackport, R., Kushner, P. J., et al. (2018). Consistency and discrepancy in the atmospheric response to Arctic sea-ice loss across climate models. *Nature Geoscience*, *11*, 155–163. https://doi.org/10.1038/s41561-018-0059-y

Screen, J. A., & Simmonds, I. (2010). The central role of diminishing sea ice in recent Arctic temperature amplification. *Nature*, *464*, 1334–1337. https://doi.org/10.1038/nature09051

Screen, J. A., & Simmonds, I. (2013). Exploring links between Arctic amplification and mid-latitude weather. *Geophysical Research Letters*, *40*, 959–964. https://doi.org/10.1002/grl.50174

Screen, J. A., & Simmonds, I. (2014). Amplified mid-latitude planetary waves favour particular regional weather extremes. *Nature Climate Change*, *4*, 704–709. https://doi.org/10.1038/nclimate2271

Sprenger, M., Fragkoulidis, G., Binder, H., Croci-Maspoli, M., Graf, P., Grams, C. M., et al. (2017). Global climatologies of Eulerian and Lagrangian flow features based on ERA-Interim. *Bulletin of the American Meteorological Society*, *98*, 1739–1748. https://doi.org/10.1175/BAMS-D-15-00299.1

Steenburgh, W. J., & Holton, J. R. (1993). On the interpretation of geopotential height tendency equations. *Monthly Weather Review*, *121*, 2642–2645. https://doi.org/10.1175/1520-0493(1993)121h2642:OTIOGHi2.0.CO;2

Sussman, H. S., Raghavendra, A., Roundy, P. E., & Dai, A. (2020). Trends in northern midlatitude atmospheric wave power from 1950 to 2099. *Climate Dynamics*, *54*, 2903–2918. https://doi.org/10.1007/s00382-020-05143-3

Taylor, P. C., Hegyi, B. M., Boeke, R. C., & Boisvert, L. N. (2018). On the increasing importance of air–sea exchanges in a thawing Arctic: A review. *Atmosphere*, *9*, 41. https://doi.org/10.3390/atmos9020041

Vavrus, S. J., Wang, F., Martin, J. E., Francis, J. A., Peings, Y., & Cattiaux, J. (2017). Changes in North American atmospheric circulation and extreme weather: Influence of Arctic amplification and Northern Hemisphere snow cover. *Journal of Climate*, *30*, 4317–4333. https://doi.org/10.1175/JCLI-D-16-0762.1

Wang, Z., Walsh, J., Szymborski, S., & Peng, M. (2020). Rapid Arctic sea ice loss on the synoptic time scale and related atmospheric circulation anomalies. *Journal of Climate*, *33*, 1597–1617. https://doi.org/10.1175/JCLI-D-19-0528.1

Wernli, H., & Papritz, L. (2018). Role of polar anticyclones and mid-latitude cyclones for Arctic summertime sea-ice melting. *Nature Geoscience*, *11*, 108–113. https://doi.org/10.1038/s41561-017-0041-0

Wirth, V., Riemer, M., Chang, E. K. M., & Martius, O. (2018). Rossby wave packets on the midlatitude waveguide—A review. *Monthly Weather Review*, *146*, 1965–2001. https://doi.org/10.1175/MWR-D-16-0483.1

Woollings, T., Barriopedro, D., Methven, J., Son, S.-W., Martius, O., Harvey, B., et al. (2018). Blocking and its response to climate change. *Current Climate Change Reports*, *4*, 287–300. https://doi.org/10.1007/s40641-018-0108-z